REVIEWS OF GEOPHYSICS AND SPACE PHYSICS, VOL. 22, NO. 2, PAGES 177–193, MAY 1984

On the Variability of the Net Longwave Radiation at the Ocean Surface

INEZ Y. FUNG

NASA Goddard Space Flight Center, Institute for Space Studies
Lamont-Doherty Geological Observatory of Columbia University

D. E. HARRISON

Center for Meteorology and Physical Oceanography, Massachusetts Institute of Technology

ANDREW A. LACIS

NASA Goddard Space Flight Center, Institute for Space Studies

The bulk formulae (BF) commonly used to estimate the net longwave radiation at the ocean surface ($LW\uparrow\downarrow$) often give dissimilar results for given surface parameters. Because the differences are climatologically significant amounts of energy, it is important to understand the sources of these differences. We present an evaluation of the most widely used BF, in terms of the assumptions made in each, the climatic conditions on which each is based, and on the results of each compared with results computed from the full radiative transfer equation (RTE) with zonally averaged atmospheric data. The differences can best be understood through examination, using the RTE as the basic tool, of the variability of $LW\uparrow\downarrow$ to variations in temperature, humidity, and cloud properties in the atmospheric column as well as at the surface. These calculations reveal that under clear sky conditions, two standard deviation perturbations of either temperature or specific humidity in the atmospheric column above the surface layer can introduce $LW\uparrow\downarrow$ variations of 30–40 W/m^2. These variations, which would be typical of the synoptic variations of $LW\uparrow\downarrow$ resulting from typical atmospheric variability, are generally greater than the differences produced by using different BF for the same surface conditions. Although the differences between BF $LW\uparrow\downarrow$ and RTE $LW\uparrow\downarrow$ can be large, the results from the Berliand and Anderson formulae duplicate the RTE clear sky $LW\uparrow\downarrow$ to ± 15 W/m^2 under a wide range of mean and perturbed conditions. The RTE studies also reveal that $LW\uparrow\downarrow$ variations due to cloudiness effects can be very large. Low clouds can reduce $LW\uparrow\downarrow$ from clear sky values by as much as 70 W/m^2. There is strong dependence of $LW\uparrow\downarrow$ on the vertical distribution of cloud properties which renders useless, for estimating instantaneous $LW\uparrow\downarrow$ under cloudy skies, the BF which do not carefully distinguish between cloud types. The accuracy of BF for climatological applications cannot be assessed without information about the geographic and temporal distributions of cloud properties. The computed sensitivity of $LW\uparrow\downarrow$ to variations in the atmospheric column illustrates the type of information and the level of accuracy necessary to attain a particular level of accuracy in $LW\uparrow\downarrow$. Improved remote sensing techniques and improved information about the cloud distribution statistics will lead to better estimates of $LW\uparrow\downarrow$ at the ocean surface and a more realistic parameterization of cloud effects in BF.

1. INTRODUCTION

The net radiation budget at the ocean surface, i.e., the difference between the net solar radiation absorbed and the net infarared (IR) radiation emitted, is an important component of the earth's climate system. This net radiative flux, together with the fluxes of sensible and latent heat, determines the heat storage and transport in the ocean, which, in turn, affect the climatic state of both the atmosphere and the ocean.

Because of the difficulty of making direct radiation measurements on shipboard, few long-term direct observations are available. Traditionally, investigators [e.g., *Clark et al.*, 1974; *Bunker*, 1976; *Wyrtki*, 1965; *Hastenrath and Lamb*, 1978] have relied on bulk formulae to evaluate the monthly mean solar and IR fluxes at the ocean surface. The bulk formulae to obtain the net solar radiation use surface albedo, cloudiness, and some estimate of the mean atmospheric turbidity or clear sky irradiance as a function of solar zenith angle or of latitude and time of year. Those formulae to obtain the net IR radiation use marine observations of sea surface temperature, near-surface air temperature and/or humidity, and cloudiness. In the atmosphere, both the solar and IR radiation incident at the surface are the integrated results of absorption, emission, and scattering in the entire inhomogeneous atmospheric column. They depend on the concentrations of all the atmospheric constituents as well as on the vertical distributions of temperature, humidity, and cloud properties. Temperature, humidity, and cloud properties each vary dramatically diurnally and seasonally, as well as on the time scales of synoptic weather systems, while the concentrations of other constituents, such as CO_2, ozone, trace gases and aerosols, vary primarily seasonally. There are also smaller, but detectable, variations in atmospheric structure and composition on interannual or longer time scales. Thus it is important to understand the variability of the radiative fluxes at the surface and to have quantitative evaluation of the bulk formulae, which use only surface and cloudiness conditions, under a wide range of atmospheric conditions.

The bulk formulae have been used widely by oceanographers and meteorologists in the study of air-sea interaction. The various bulk formulae calculations of climatological radiative fluxes agree with one another in the general patterns of temporal and spatial variations of the fluxes, but the magnitudes differ substantially. For example, the annual mean net all-wave radiation gain over the tropical Atlantic Ocean as estimated by *Bunker* [1976] is consistently higher, by 30

Paper number 4R0239.
0034-6853/84/004R-0239$15.00

TABLE 1*a*. List of Commonly Used Bulk Formulae for Net Longwave Radiation at the Surface

Reference	Formula
Brunt [1932]	$\varepsilon\sigma T_s^4[0.39 - 0.05(e_a)^{1/2}]F(C)$
Berliand and Berliand [1952]	$\varepsilon\sigma T_a^4[0.39 - 0.05(e_a)^{1/2}]F(C) + 4\varepsilon\sigma T_a^3(T_s - T_a)$
Clark et al. [1974]	$\varepsilon\sigma T_s^4[0.39 - 0.05(e_a)^{1/2}]F(C) + 4\varepsilon\sigma T_s^3(T_s - T_a)$
*Hastenrath and Lamb** [1978]	$\varepsilon\sigma T_s^4[0.39 - 0.056(q_a)^{1/2}]F(C) + 4\varepsilon\sigma T_s^3(T_s - T_a)$
Efimova [1961]	$\varepsilon\sigma T_a^4(0.254 - 0.00495e_a)F(C)$
Bunker [1976]	$0.022[\varepsilon\sigma T_a^4(11.7 - 0.23e_a)F(C)] + 4\varepsilon\sigma T_a^3(T_s - T_a)$
Anderson [1952]	$\varepsilon\sigma[T_s^4 - T_a^4(0.74 + 0.0049e_a)]F(C)$
Swinbank [1963]	$\varepsilon\sigma(T_s^4 - 9.36 \times 10^{-6} T_a^6)F(C)$

Here ε is the emissivity of the ocean surface, taken to be 1 in these calculations; σ is the Stefan-Boltzmann constant, equal to 567×10^{-10} W m^{-2} K^{-4}; T_s is the sea surface temperature (in kelvins); T_a is the near-surface air temperature (in kelvins); e_a is the near-surface vapor pressure (in millibars); $F(C)$ is the cloud correction factor summarized in Table 1*b*.

*q_a is assumed to be q (1000 mbar) and is related to e_a via equation (15*b*).

W/m^2 or more, than that estimated by *Hastenrath and Lamb* [1978]. These differences arise out of selecting different bulk formulae and/or out of different data processing procedures.

The GARP Atlantic Tropical Experiment (GATE) provided a useful data set for the evaluation of the heat fluxes at the ocean surface. Simple models of radiative transfer were used to calculate the upward and downward solar and IR fluxes at the ocean surface from the GATE data [*Duing et al.*, 1980], with some surprising and disturbing results. The net solar flux averaged for each set of ship data varied by as much as 60 W/m^2 from ship to ship within the B/C scale region (about 1000 km × 1000 km) within each phase (10–20 days) of the experiment; the average IR flux varied by 30 W/m^2. These variations in the radiative fluxes, together with the variations in latent and sensible heat fluxes, resulted in net heat fluxes which were of opposite signs within a phase of GATE. Mesoscale and small-scale variations in cloudiness and other meteorological parameters may contribute to the large differences in the average fluxes [*Weare and Strub*, 1981], but these large differences among calculations based on much better observations than will be routinely available in the next few years are disturbing. The difference represents physically important amounts of heat. An uncertainty in the net heat flux of 30 W/m^2 over the tropical oceans, like that found in the net IR flux during GATE, will lead to an uncertainty in the inferred ocean total meridional heat transport of the order of 10^{15} W, which is the same order as the estimated maximum heat transport itself (see, e.g., *Oort and Vonder Haar* [1976]).

Recently, satellite measurements of the radiation balance at the top of the atmosphere, together with information about heat storage and flux divergence in the atmosphere, have allowed the inference of the energy balance at the ocean surface [*Oort and Vonder Haar*, 1976; *Stevens et al.*, 1981]. Inaccuracy in the satellite measurements as well as uncertainties in the magnitudes of the atmospheric heat flux divergence will lead to uncertainties in the surface heat balance. *Oort and Vonder Haar* [1976] estimate that these uncertainties in surface heat balance are about ±20 W/m^2 in the tropics and about ±50 W/m^2 at high latitudes.

How well must the net surface energy flux be known in order that scientifically important questions can be addressed? A recent design study for a tropical upper ocean field program concludes that the maximum allowable error in monthly means is 20 W m^{-2} [*Niiler*, 1982]. Various criteria have been suggested for typical middle-latitude values, but 10 to 20 W m^{-2} again appears to be the maximum allowable error. In terms of surface-flux-induced ocean mixed layer temperature changes, an error in flux of 20 W m^{-2} produces an error in mixed layer heating rate of 0.7°C/month if the mixed layer is 20 m deep; this is larger than, or a significant fraction of, the normal seasonal heating rate over much of the ocean.

In order to attain the desired ±10 W/m^2 accuracy in the net surface heat budget, it is important to know and to understand the uncertainties in the individual components that make up the surface heat budget. *Gautier et al.* [1980] have described a technique for deducing the net solar radiation at the surface from satellite measurements. Preliminary results from their method have led to claims that, with adequate calibration data sets, it may be possible to determine the monthly mean solar flux to within ±10 W/m^2. However, there is no similar or comparable technique of estimating the net IR flux at the surface. It seems that meteorologists and oceanographers will continue to rely on bulk formulae to estimate the net IR flux for some time to come.

In this paper we present a systematic evaluation of the bulk formulae used to determine the net IR flux at the ocean surface, based on comparison of their results with IR fluxes computed from the full radiative transfer equation (RTE) and zonally averaged atmospheric data. We emphasize the sensitivity of the net IR radiation to variations in the atmospheric column above the surface. We do not assert that the IR fluxes obtained from the radiative transfer calculations are "truth" or that the bulk formulae results which differ from the radiative calculations results are incorrect. However, we believe that the RTE solutions accurately reflect the changes in radiative fluxes that result from perturbations of the input variables, and we feel it is proper to prefer those bulk formulae that reproduce the trends of the changes over those which do not.

Section 2 summarizes the bulk formulae we have chosen for investigation. We provide a brief review of the physics of the radiative transfer equation in section 3 and the method used in the investigation in section 4. Section 5 presents our clear sky IR results, and sections 6 and 7 present our results concerning the effects of cloudiness and inversion on net IR flux at the ocean surface. We conclude in section 8 with a discussion of these results and a summary of their implications for data requirements for improved estimates of the ocean net IR flux.

2. BULK FORMULAE

The net IR flux at the surface ($LW\uparrow\downarrow$) is the difference between the upward IR radiation ($LW\uparrow$) emitted by the surface and the downward IR radiation ($LW\downarrow$) from the atmosphere:

$$LW\uparrow\downarrow = LW\uparrow - LW\downarrow \tag{1}$$

The upward flux can be adequately given by $\varepsilon\sigma T_s^4$, where ε is the emissivity of the surface, σ is the Stefan-Boltzmann constant, and T_{s*} is the temperature of the emitting surface. The physics is simply blackbody radiation, but there can be significant differences between T_{s*} and the sea surface temperature T_s measured by a bucket or intake temperature (see, e.g., *Miyakoda and Rosati* [1982]). Furthermore, estimates of ε vary from 0.93 to 1.0 (see, e.g., *Anderson* [1952]). The calculation of the downflux is much more complicated, as will become clear in our discussion of the RTE (section 3). However, all the bulk

TABLE 1b. Cloud Correction Factor $F(C)$

Reference	Formula	a or b*									
		80°N	70°N	60°N	50°N	40°N	30°N	20°N	10°N	5°N	Equator
Clark et al. [1974]	$F(C) = 1 - bC^2$				0.73	0.69	0.64	0.60	0.56	0.53	0.51
Bunker [1976]	$F(C) = 1 - aC$	0.84	0.80	0.76	0.72	0.68	0.63	0.59	0.52	0.50	
Hastenrath and Lamb [1978]	$F(C) = 1 - bC^2$						0.53				

*Values in the southern hemisphere are the same as those at the same latitude in the northern hemisphere.

formulae assume that the clear sky downflux, and hence the net IR flux, can be determined from some combination of T_s, T_a (the near-surface air temperature), and e_a (the near-surface water vapor pressure).

When $T_a = T_s = T$, the bulk formulae for clear sky conditions generally assume the form

$$LW\uparrow\downarrow = I_0(T) = \varepsilon\sigma T^4 f(e_a) \tag{2}$$

Table 1*a* lists eight commonly referenced bulk formulae grouped according to their functional form of $f(e_a)$. Using observations for Benson (England), *Brunt* [1932] suggested that the downflux depends on the square root of e_a. *Efimova* [1961] found that during the International Geophysical Year (1957) the monthly mean net fluxes at 24 Soviet stations depended linearly on e_a. *Swinbank* [1963], on the other hand, claims that e_a is strongly correlated with T_a and obtains a relationship between the downflux and T_a alone. Swinbank's data came mainly from Aspendale (near Melbourne), with five observations from Kerang (about 200 miles inland from Melbourne) and six observations in the tropical Indian Ocean.

To account for situations when $T_a \neq T_s$, investigators subsequently included both T_a and T_s in their formulae. *Berliand and Berliand* [1952] added a temperature jump correction term CORR(T) to the Brunt formula:

$$LW\uparrow\downarrow = I_0(T) + \mathrm{CORR}(T) \tag{3}$$

A similar correction term was added to the Brunt formula to yield the formula used by Clark and to the Efimova formula to yield the formula used by Bunker. CORR(T) is strictly $\varepsilon\sigma(T_s^4 - T_a^4)$ and is approximated either as

$$\mathrm{CORR}(T_a) = 4\varepsilon\sigma T_a^3(T_s - T_a) \tag{4}$$

or as

$$\mathrm{CORR}(T_s) = 4\varepsilon\sigma T_s(T_s - T_a) \tag{5}$$

Both CORR(T_a) and CORR(T_s) have been commonly used.

The dichotomy between the use of T_a versus T_s arises in the formula for I_0 as well. A strict extension of the original formulae requires $I_0(T_a)$ rather than $I_0(T_s)$. There is no clear choice for either, mainly because the difference is small for many commonly encountered situations and is not easily resolvable. A mid-latitude springtime example, $T_a = 270$ K and $T_s = 280$ K, however, illustrates that the difference can be important; taking T_s instead of T_a in I_0 in (3) for this example changes I_0 by 16% or roughly 10 W/m^2. Apart from the fact that many of the original formulae correlated the downflux with σT_a^4, there seems to be little rationale to preferring T_a over T_s in I_0. Nevertheless, we must recognize the further uncertainties introduced in the formulae.

While the functional forms of the bulk formulae all appear to capture the temperature and water vapor effects on $LW\uparrow\downarrow$, they differ mainly in the values of the constant coefficients. The constants in the formulae are obtained by regression fitting of the chosen formula to specific sets of observations. The same formula can be fitted, perhaps equally successfully, to different sets of observations, resulting in new values of the constant coefficients. Indeed *Brunt* [1939] (see also *Kondratyev* [1969]) shows a table of empirical constants obtained by matching observations with the Brunt-type formula and the range of e_a for each set of observations. For similar ranges of e_a, these empirical constants vary by 50% or more. Instrumental differences may contribute to the wide range of constants obtained under similar surface conditions, but the contributions from conditions aloft cannot be assessed.

Similarly, different formulae may be applied to the same set of observations with comparable success. Anderson fitted four bulk formulae, among them a Brunt-type and an Efimova-type formula, to his observations of $LW\uparrow\downarrow$ made at Lake Hefner, Oklahoma. He found, for the atmospheric conditions at Lake Hefner (3 mbar $< e_a <$ 30 mbar), that the differences in $LW\uparrow\downarrow$ estimated from the resultant formulae were small, in fact, smaller than the scatter of the observations. Anderson chose an Efimova-type straight line fit because of its simplicity.

Clearly, because the bulk formulae are obtained by statistical fitting of a large number of observations, individual observations will often not fall on the regression line. Departures can be substantial [e.g., *Anderson*, 1952]. Recently, *Reed and Halpern* [1975], *Reed* [1976], and *Simpson and Paulson* [1979] have compared a few direct and rather short duration (several days) oceanic observations of net IR flux with those computed from the bulk formulae. Their observations were made in the mid-latitude eastern Pacific. *Reed and Halpern* [1975] found that Anderson's formula gave the best fit to their summertime observations. Both *Reed* [1976] and *Simpson and Paulson* [1979] found that Efimova's formula gave the lowest estimate of net IR flux of all the bulk formulae they investigated. However, Reed preferred Efimova's formula for spring/autumn conditions, and Simpson and Paulson rejected Efimova's formula for giving the largest underestimate of net IR flux under winter conditions. Reed and Halpern also found that Berliand's formula gave better agreement with observations if CORR(T_s) is omitted except when $T_s < T_a$. We shall comment on these results in section 5.

The effect of cloudiness on the net IR flux at the surface is generally parameterized by a cloudiness correction factor $F(C)$ of the type $(1 - aC^m)$, where C is the fraction of cloud cover, a may be a latitudinally varying constant, and m is a constant which varies between 1 and 2. Where observations of clouds differentiate between low, middle, and high clouds, investigators [e.g., *Efimova*, 1939; *Galperin*, 1949; *Levastu*, 1967; *Reed*, 1976] choose values of a for each cloud type. However, such cloud information is not routinely available from surface

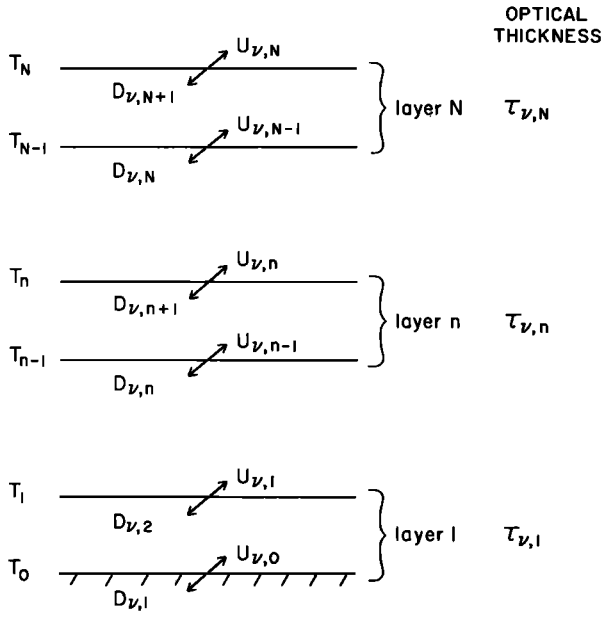

Fig. 1. Schematic diagram of vertical structure of the radiative transfer model.

marine observations, and a single cloudiness correction factor is generally used, where C is then the total cloudiness. In practice, some investigators [e.g., *Budyko*, 1964] use a linear factor $1 - aC$, while others [e.g., *Clark et al.*, 1974; *Hastenrath and Lamb*, 1978] use a quadratic factor $1 - bC^2$, where a and b are latitudinally dependent constants.

$F(C)$ used by Clark, Hastenrath, and Bunker are summarized in Table 1*b*. The latitudinal variation of the coefficients should represent, in some way, the latitudinal variations of "typical" or "averaged" cloud types. Note that for the same value of fractional cloud cover C, $F(C)$ is larger at low latitudes than at high latitudes, suggesting that the "typical" high-latitude cloud has a larger impact on $LW\uparrow\downarrow$ than the "typical" low-latitude cloud. This will be discussed in section 6.3. Note also that the coefficients used in the formulae are very similar. Clark and Hastenrath use the quadratic form of $F(C)$, while Bunker uses the linear form, leading to very different values of $LW\uparrow\downarrow$ for the same fractional cloud cover. This may be a partial explanation for the high values of $LW\uparrow\downarrow$ obtained by Bunker.

As the bulk formulae were developed from continental data obtained prior to the 1960's, their direct application to evaluate the net IR flux from the ocean is questionable, as is suggested by the differing conclusions of Reed and Halpern, Reed, and Simpson and Paulson. Furthermore, the (in)accuracy of antiquated instruments, the different measurement methods, and the sparsity of observation have prevented the universal validation of these formulae. These considerations led *Kondrateyev* [1969] and *Budyko* [1974] to conclude that the formulae may be useful for estimates of large-area, long-term means but are probably not suitable for comparison with specific measurements of short duration (a few days) at a given site. *Anderson* [1952] has also emphasized this same point, based simply on the data scatter about his parameterization curve.

3. Radiative Transfer Calculations

The radiative transfer equation (RTE) states that the energy radiated by a parcel of material in a particular frequency interval and particular direction (denoted by an increment of solid angle around the direction) is the sum of the energy transmitted through the parcel and the energy emitted from within the parcel, in that frequency interval and direction. The total radiation is obtained by integrating over all solid angles and frequencies. The physics of radiative transfer is well understood conceptually, and the radiative properties of most of the constituents of the atmosphere are well known. However, the radiative calculations become extremely involved when, as in the atmosphere, many constituents are present and the radiative properties of the atmosphere vary in space and time. Approximations must be made to simplify the calculations if the radiative solution is to be obtained efficiently and repeatedly for changing conditions, as it must be in atmospheric circulation and climate models. The reader is referred to *Tiwari* [1978] for an excellent critical review of the different line and band models for infrared absorption.

The RTE calculation procedure described here was developed for use in the three-dimensional global climate model at the Goddard Institute for Space Studies [*Hansen et al.*, 1983]. The calculations evaluate the effects of changes in atmospheric temperature, humidity, cloud, aerosol distribution, and chemical composition. Longwave radiation calculations include all the major absorption bands of CO_2, H_2O, and O_3 as well as the weaker bands of CO_2, N_2O, and CH_4. The continuum absorption by water vapor, including the self-broadening dimer "*e*-type" absorption, is also evaluated. It is difficult to obtain the information necessary to compare our RTE solution directly with atmospheric radiation observations because the atmospheric column is seldom adequately sampled at a time when direct radiation measurements are being made. However, a comparison of the results from the radiative transfer model with those from a detailed line-by-line calculation shows that the model heating/cooling rates are good to at least 1% [*Lacis et al.*, 1979]. The method of calculation is outlined below. Basic background information on blackbody radiation, the RTE, line/band approximations, etc., can be found in the work of *Liou* [1980], *Houghton* [1977], or *Tiwari* [1978].

We consider an atmospheric column of N plane parallel layers, each denoted by subscript n, $n = 1, 2, \cdots, N$ (Figure 1). In this study, $N = 10$; the layering corresponds to that of the data of *Oort and Rasmusson* [1971]. Temperatures T_n, $n = 0, 1, 2, \cdots, N$, are defined at layer edges. The mean optical thickness for the nth layer at a particular frequency ν is $\tau_{\nu,n}$. At frequency ν and beam angle θ the upward IR irradiance $U_{\nu,n}$ and the downward IR irradiance $D_{\nu,n}$ at the edges of the layer n are given by

$$U_{\nu,n} = U_{\nu,n-1}e^{-\tau_{\nu,n}/\mu} + E_{\nu,n}{}^{\uparrow} \tag{6}$$

$$D_{\nu,n} = D_{\nu,n+1}e^{-\tau_{\nu,n}/\mu} + E_{\nu,n}{}^{\downarrow} \tag{7}$$

where $\mu = \cos\theta$. The first terms on the right-hand side of (6) and (7) are the transmitted IR irradiances given by Lambert's law [*Liou*, 1980], and the second terms are the IR irradiances emitted in the layer:

$$E_{\nu,n}{}^{\uparrow} = \int_0^{\tau_{\nu,n}} B_{\nu,n}(\tau') \exp\left[-(\tau_{\nu,n} - \tau')/\mu\right] \frac{d\tau'}{\mu} \tag{8}$$

$$E_{\nu,n}{}^{\downarrow} = \int_0^{\tau_{\nu,n}} B_{\nu,n}(\tau') e^{-\tau'/\mu} \frac{d\tau'}{\mu} \tag{9}$$

where $B_{\nu,n}$ is the Planck function at frequency ν and temperature T_n.

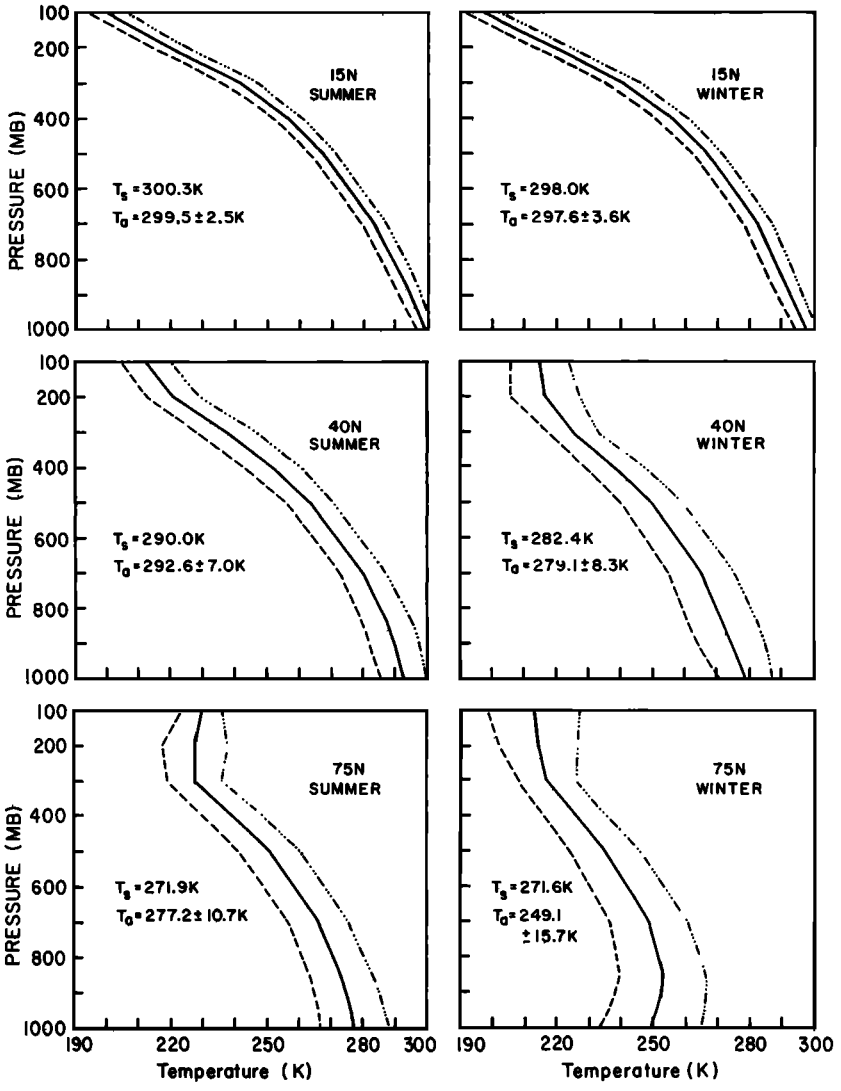

Fig. 2*a*. Vertical profiles of temperatures under mean (solid line), hot (dot-dash line), and cold (dashed line) conditions for the six environments. Data are from *Oort and Rasmusson* [1971]. Sea surface temperatures for each environment are taken from *Alexander and Mobley* [1976].

The boundary conditions are given by

$$D_{\nu,N+1} = 0 \tag{10a}$$

$$U_{\nu,0} = \varepsilon_\nu B_{\nu,0} + \alpha_\nu D_{\nu,1} \tag{10b}$$

α_ν and $\varepsilon_\nu = 1 - \alpha_\nu$ are the albedo and emissivity of the ocean surface, respectively. Equation (10*a*) states that there is no downward IR flux at the top of the atmosphere. Equation (10*b*) states that the upflux at the ocean surface is given by the sum of the emission from the ocean surface plus the reflection of the downward flux. The albedo α_ν of the ocean surface is parameterized as a function of frequency and surface wind speed. Although α_ν ranges from 4% to 10%, variations in $LW\uparrow$ are generally less than 5 W/m^2, since variations in the reflected component $\alpha_\nu D_{\nu,1}$ in (10*b*) nearly compensates for the variations in the emitted component $\varepsilon_\nu B_{\nu,0}$.

For the frequency interval (ν_a, ν_b), the total upward U_n and downward D_n IR fluxes are then obtained by integrating $U_{\nu,n}$ and $D_{\nu,n}$ overall frequencies in (ν_a, ν_b) and beam angles:

$$U_n = \int_0^{\pi} d\theta \int_{\nu_a}^{\nu_b} U_{\nu,n} \cos\theta \, d\nu \tag{11}$$

$$D_n = \int_{-\pi}^{0} d\theta \int_{\nu_a}^{\nu_b} D_{\nu,n} \cos\theta \, d\nu \tag{12}$$

Computationally, a direct numerical solution of (6) to (12) is extremely difficult because of the spectral complexity of the atmospheric constituents and the vertically inhomogeneous and complex chemical composition of the atmosphere. The optical thickness at a given temperature and pressure level is determined by all the absorption processes of the atmosphere, and absorption coefficients vary greatly with frequency. The properties of the more than 10^5 lines in the atmospheric spectrum are well-known functions of temperature and pressure, so that a line-by-line calculation is possible, but it is very cumbersome to carry out. The basic problem then is to find an accurate yet tractable way to calculate the changes in absorption properties of each constituent. To do this, *Lacis et al.* [1979] devised the correlated k distribution method, which is a generalization of the k distribution method of *Lacis and Hansen* [1974]. The approach taken in this method is summarized in the appendix. The reader is referred to *Lacis et al.* [1979] for a detailed discussion of the method and for a comparison of the correlated k distribution method with line-by-line calculations.

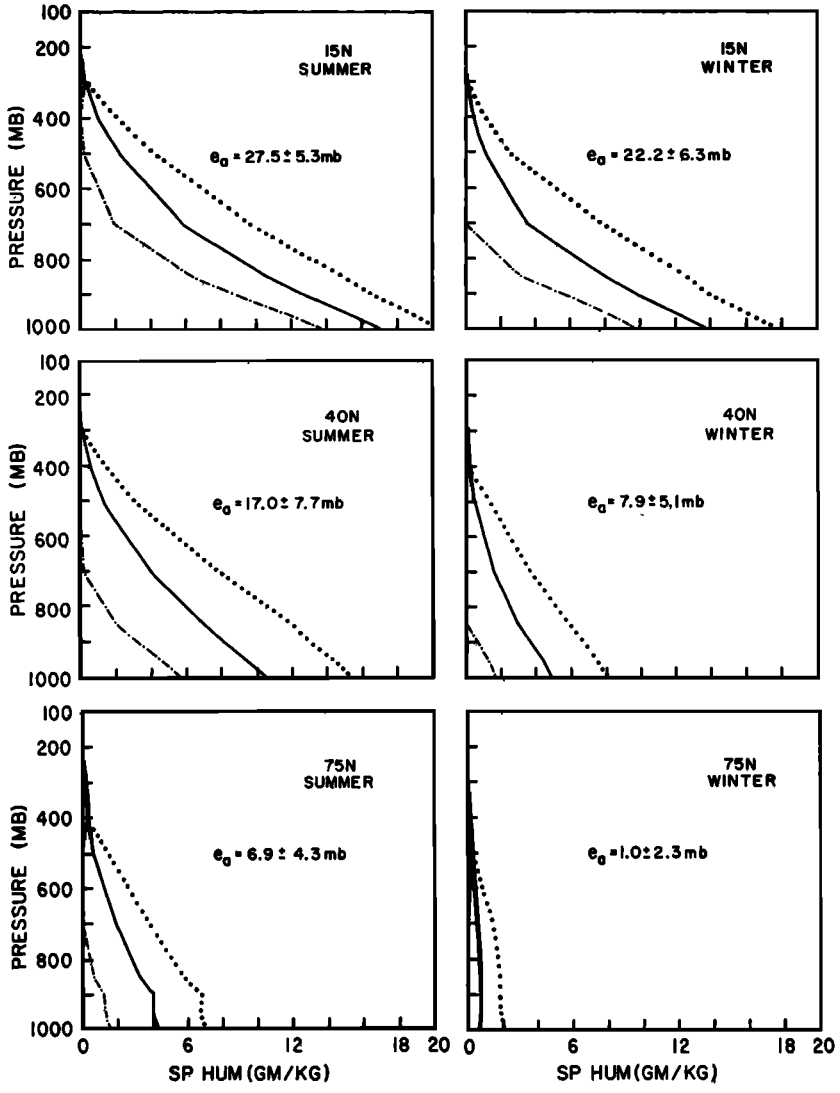

Fig. 2*b*. Vertical profiles of specific humidity under mean (solid line), wet (dotted line), and dry (dash-dot line) conditions for the six environments. Data are from *Oort and Rasmusson* [1971].

In the cloudy sky calculations, cloud optical thicknesses $\tau_{c,n}$ are specified for layers in which clouds are assumed to be present. We take the size of water droplets to be 10 μm and that of ice particles to be 25 μm. The specified $\tau_{c,n}$ is taken to be the optical thickness in the visible spectrum, at 0.55 μm. The optical thicknesses at other wavelengths (or frequencies) are obtained from Mie scattering cross sections relative to that at 0.55 μm. These "cloudy" absorption coefficients are then used in the correlated k distribution method discussed above to determine the upward and downward IR fluxes at the edge of each layer.

The thermal radiation calculations are performed with the nonscattering assumption (single-scattering albedo is 0). The effect of multiple scattering, which is small for thermal radiation, is included in parameterized form as an effective emissivity of the clouds. Off-line multiple-scattering calculations [cf. *Hansen and Travis*, 1974] are performed for frequencies in the infrared regime to obtain the cloud reflectivity (albedo) as a function of wavelength. The flux emitted by clouds is then corrected as in (10*b*) for the ocean surface.

4. METHOD

The lack of global observations of net IR radiation at the surface contemporaneous with observations of vertical profiles of temperature, humidity, and cloud radiative properties prevents us from a direct investigation of the sensitivity of $LW\uparrow\downarrow$ and evaluation of the bulk formulae. The radiative transfer model, in which atmospheric structure and composition can be independently specified, provides us with an alternate means to carry out our investigation.

We evaluate the net IR radiation at the ocean surface as determined by the radiative transfer equations (section 3) and by the bulk formulae listed in Table 1*a*. Results for clear sky are presented in section 5, for cloudy sky in section 6, and for a tropical case with an inversion in section 7.

The net longwave radiation at the surface is computed for six environments: summer and winter conditions in the tropics (15°N), mid-latitudes (40°N), and the subarctic (75°N). For each environment we have considered five combinations of vertical profiles of temperature $T(p)$ and specific humidity $q(p)$

as a function of pressure p:

$$T(p) = \langle T(p)\rangle + T'(p) \qquad q(p) = \langle q(p)\rangle + q'(p) \tag{13}$$

Mean

$$T'(p) = 0 \qquad q'(p) = 0 \tag{14a}$$

Cold

$$T'(p) = -2\sigma_T(p) \qquad q'(p) = 0 \tag{14b}$$

Hot

$$T'(p) = 2\sigma_T(p) \qquad q'(p) = 0 \tag{14c}$$

Dry

$$T'(p) = 0 \qquad q'(p) = -2\sigma_q(p) \tag{14d}$$

Wet

$$T'(p) = 0 \qquad q'(p) = 2\sigma_q(p) \tag{14e}$$

Here $\langle T(p)\rangle$, $\langle q(p)\rangle$, $\sigma_T(p)$, and $\sigma_q(p)$ for each season and latitude are taken from the zonally averaged mean and transient eddy statistics of *Oort and Rasmusson* [1971] and are illustrated in Figure 2. Because the observation sites are mainly land based, the profiles may not be typically oceanic profiles. However, *Bunker* [1976] shows a range of oceanic air-sea temperature values which generally bracket the mean conditions used here. Except in certain regions, such as the Gulf Stream, $\sigma_T(p)$ and $\sigma_q(p)$ over the ocean are typically not as large as those over land. It is not clear if an inversion suggested in the subarctic profiles exists over the ocean. However, these profiles are the only large-scale atmospheric statistics that are not site specific and that are clearly documented. We can also view $\sigma_T(p)$ and $\sigma_q(p)$ as measurement uncertainties in $T(p)$ and $q(p)$ or as uncertainties introduced by retrieval procedures from satellite data. Whatever the limitations introduced by these profiles, the calculations will provide information about the sensitivity of $LW\uparrow\downarrow$ to changes in and uncertainties about the atmospheric column and the ability of the bulk formulae to reproduce them. Mean sea surface temperatures for each season and latitude are taken from the data of *Alexander and Mobley* [1976] and are included in Figure 2*a*.

For these calculations the ozone concentration is taken from the climatologic data of *Park and London* [1974] and includes seasonal, latitudinal, and altitudinal variations. The concentrations of the minor gas absorbers are assumed to be at their climatological values.

We have assumed that the CO_2 concentration in the atmosphere is 315 ppm. Observations of CO_2 concentration at Mauna Loa Observatory and at other CO_2 monitoring stations clearly show that the concentration of CO_2 in the atmosphere is increasing steadily at a rate of ~ 1.5 ppm yr^{-1} and that there are seasonal oscillations with peak-to-trough amplitudes as large as ~ 15 ppm at Point Barrow, Alaska [*Keeling*, 1982]. The value of 315 ppm we have assumed in these calculations is representive of the annual mean CO_2 concentration in 1958. That these variations of atmospheric CO_2 should have small impact on the $LW\uparrow\downarrow$ at the ocean surface is illustrated by one-dimensional radiative-convective model calculations where the CO_2 concentration in the atmosphere is artificially increased from 300 ppm to 600 ppm. These calculations show that the resultant change in the net radiative flux at the surface is only 1–2 W/m^2 due to the increase in CO_2 alone (i.e., without feedbacks of the hydrologic cycle).

TABLE 2. $LW\uparrow\downarrow$ at the Surface Under Clear Skies as Determined by the RTE

	15°N		40°N		75°N	
	Summer	Winter	Summer	Winter	Summer	Winter
Mean	60	72	54	98	54	147
Hot	46	55	22	66	17	113
Cold	72	87	82	126	85	175
Dry	83	102	92	138	85	182
Wet	43	48	28	77	35	134

Units are in watts per square meter.

TABLE 3. Departure of LW (Bulk Formula) From LW (RTE) for Six Mean Environments Under Clear Skies

	15°N		40°N		75°N	
	Summer	Winter	Summer	Winter	Summer	Winter
Brunt	−3	−4	18	−11	24	−45
Berliand	2	−2	4	1	6	1
Clark	3	−2	6	5	1	54
Hastenrath	16	10	13	11	5	56
Efimova	−8	−9	14	−26	17	−95
Bunker	0	−3	5	−6	−2	−15
Anderson	1	−4	3	−8	−4	−6
Swinbank	17	6	13	9	14	29

Units are in watts per square meter.

In the calculation of $LW\uparrow\downarrow$ in the bulk formulae, we have assumed that

$$T_a = T(1000 \text{ mbar}) \tag{15a}$$

and

$$e_a = q(1000 \text{ mbar}) \times p_s/\gamma \tag{15b}$$

where $p_s (= 1000$ mbar) is the surface pressure and γ ($=0.622$) is the ratio of molecular weight of water to the molecular weight of dry air.

5. Clear Sky Results

5.1. *RTE Results for Clear Sky*

Table 2 summarizes the $LW\uparrow\downarrow$ from the RTE for clear sky conditions. As has been noted by other investigators [e.g., *Bunker*, 1976], there is little latitudinal gradient of $LW\uparrow\downarrow$ under mean summer conditions. $LW\uparrow\downarrow$ is about 55 ± 15 W/m^2 from 15°N to 75°N. Under mean winter conditions, however, $LW\uparrow\downarrow$ varies between 72 and 147 W/m^2. In the subarctic the reduction in $LW\downarrow$ due to lower air temperature and humidity far exceeds the reduction in $LW\uparrow$ due to lowered sea surface temperature, so that $LW\uparrow\downarrow$ in the subarctic winter is double that in the tropical winter.

Similarly, when the atmospheric column is hot or wet, the increased downflux results in a reduced $LW\uparrow\downarrow$. The reverse is true when the conditions are cold or dry. Given these two standard deviation perturbation profiles, Table 2 shows that $LW\uparrow\downarrow$ ranges between 43 and 83 W/m^2 in the summer tropics, between 48 and 102 W/m^2 in the winter tropics, between 22 and 92 W/m^2 in the summer mid-latitudes, between 66 and 138 W/m^2 in the winter mid-latitudes, between 17 and 85 W/m^2 in the summer subarctic, and between 113 and 182 W/m^2 in the winter subarctic. Of course, temperature and humidity changes generally occur concurrently; specific hu-

TABLE 4. Anomalous Net Longwave Radiation Under Clear Sky Cold Atmospheric Conditions in the Six Environments as Estimated by RTE and the Bulk Formulae

	15°N		40°N		75°N	
	Summer	Winter	Summer	Winter	Summer	Winter
RTE	12	15	28	28	31	28
Brunt	0	0	0	0	0	0
Berliand	13	17	30	25	35	14
Clark	15	21	37	41	47	69
Hastenrath	15	21	37	41	47	69
Efimova	−2	−3	−6	−8	−10	−12
Bunker	13	17	30	26	36	17
Anderson	13	17	31	30	37	36
Swinbank	18	25	44	40	49	40

Units are in watts per square meter.

midity tends to increase when temperature increases. This will further increase $LW\downarrow$ and reduce $LW\uparrow\downarrow$. Hence the results given here represent a conservative estimate of the range of instantaneous $LW\uparrow\downarrow$ at the ocean surface.

5.2. *Bulk Formulae Results for Mean Clear Sky Conditions*

Table 3 compares $LW\uparrow\downarrow$ computed from the bulk formulae with those computed from the RTE for the mean environments. To simplify the discussion below, we shall use *LW* (formula) to denote the mean $LW\uparrow\downarrow$ at the surface computed from a bulk formula, *LW* (RTE) to denote the mean $LW\uparrow\downarrow$ at the surface computed from the RTE, and ΔLW (formula) = *LW* (formula) − *LW* (RTE) to denote the difference in mean $LW\uparrow\downarrow$ as determined by the two methods.

Table 3 shows ΔLW for the eight bulk formulae listed in Table 1*a* for the six mean environments. *LW* (Berliand) and *LW* (Anderson) come within 10 W/m^2 of *LW* (RTE) for all six mean environments. Except for subarctic winter, *LW* (Clark) and *LW* (Bunker) are also within 10 W/m^2 of *LW* (RTE). *LW* (Hastenrath) and *LW* (Swinbank) are higher than *LW* (RTE). ΔLW (Hastenrath) and ΔLW (Swinbank) are as large as 16 W/m^2 in the tropical summer.

The two groups of formulae, Brunt-Berliand-Clark and Efimova-Bunker, allow us to examine the effect of the temperature jump correction CORR(T) and the use of T_a versus T_s in I_0 (equation (3)) on the $LW\uparrow\downarrow$. The omission of the temperature jump correction in the Brunt and Efimova formulae results in the largest disagreement, within each group, with the RTE. With CORR(T) the improved agreement with the RTE is large in the mid-latitude summer and subarctic summer when $T_a > T_s$, consistent with the findings of *Reed and Halpern* [1975]. However, even when $T_a < T_s$, as in mid-latitude winter and subarctic winter, the Berliand and Bunker formulae (which use CORR(T_a)) show significant improvement over the Brunt and Efimova formulae, respectively. The difference resulting from the use of $I_0(T_a)$ instead of $I_0(T_s)$ can be seen in the comparison of the Berliand and Clark formulae. When $T_s - T_a$ is small, as in the tropics, the difference between the Berliand and Clark formulae is less than 5 W/m^2 and is probably insignificant. However, in the subarctic winter, when $T_s - T_a = 22$ K, the Berliand and Bunker formulae with $I_0(T_a)$ and CORR(T_a) show a markedly better agreement with RTE than the other formulae in their respective groups.

5.3. *Bulk Formulae Results for Perturbed Clear Sky Conditions*

The departures of the net surface heat flux from its climatological mean is an important cause and indicator of changes in SST as well as in the climatic states of the atmosphere and the ocean. Changes in $LW\uparrow\downarrow$ may result from changes in SST or from changes in the atmospheric column. Because the bulk formulae have been used, and will continue to be used, to estimate the mean and anomalous $LW\uparrow\downarrow$, it is important to know if the bulk formulae do capture the sensitivity in $LW\uparrow\downarrow$ in response to departures from mean conditions.

To investigate the sensitivity of $LW\uparrow\downarrow$ to changes in the atmospheric column, we have kept SST's at their mean values (see Figure 2) and perturbed the atmospheric column according to (14).

Let

$$\delta LW \text{ (formula or RTE)} = LW\uparrow\downarrow(T, q) - LW\uparrow\downarrow(\bar{T}, \bar{q})$$

be the anomalous $LW\uparrow\downarrow$, estimated by the same formula or method, that results from perturbed temperature or humidity conditions. Tables 4 to 7 show δLW for the six environments, as determined by the bulk formulae and by the RTE. A preferred formula, of course, is one which can duplicate both the mean $LW\uparrow\downarrow$ and its sensitivity as estimated by the RTE (cf. Table 2). Actual departures of the bulk formulae $LW\uparrow\downarrow$ from the RTE $LW\uparrow\downarrow$ can be computed from δLW (formula) + ΔLW (formula) − δLW (RTE).

When temperature in the atmospheric column is perturbed by $\pm 2\sigma_T$ (cf. Tables 4 and 5), δLW (RTE) ranges from −17 to +15 W/m^2 in the tropics, from −32 to +28 W/m^2 in mid-latitudes, and from −36 to +31 W/m^2 in the subarctic.

With these temperature perturbations, δLW from the Anderson, Berliand, and Bunker formulae are within 5 W/m^2 of δLW (RTE) in the tropics and mid-latitudes. These formulae disagree most with the RTE calculations in the subarctic. Even there, the difference is ≤ 15 W/m^2. The difference between the use of T_a and T_s in I_0 (cf. (2)) again shows up in a comparison of the δLW from the Berliand and Clark formulae. δLW (Berliand), except in subarctic winter, is closer than δLW (Clark) to δLW (RTE). The Clark formula gives larger δLW than the Berliand formulae and the RTE to temperature perturbations. Efimova's formula shows the opposite sensitivity to temperature changes: decreasing T_a in Efimova's formula results in decreased δLW. When the surface temperature jump correction CORR(T_a) is added to the Efimova formula, i.e., the Bunker formula, δLW (Bunker) is, again except in the subarctic, within 5 W/m^2 of δLW (RTE). Swinbank's formula

TABLE 5. Like Table 4, Except for Hot Atmospheric Conditions

	15°N		40°N		75°N	
	Summer	Winter	Summer	Winter	Summer	Winter
RTE	−14	−17	−32	−32	−36	−34
Brunt	0	0	0	0	0	0
Berliand	−13	−18	−35	−32	−45	−29
Clark	−15	−21	−37	−41	−47	−69
Hastenrath	−15	−21	−37	−41	−47	−69
Efimova	2	3	7	9	12	15
Bunker	−13	−18	−35	−32	−47	−33
Anderson	−13	−18	−33	−32	−41	−44
Swinbank	−19	−27	−49	−47	−59	−54

Units are in watts per square meter.

shows larger δLW than δLW (RTE). This is not surprising, since Swinbank assumed that temperature perturbations would be accompanied by humidity perturbations, which are omitted in these calculations in Tables 4 and 5. The Brunt formula has no dependence on T_a and therefore no sensitivity to temperature changes.

When humidity in the atmospheric column is perturbed by $\pm 2\sigma_q$ (Tables 6 and 7), δLW (RTE) may range from -23 to $+30$ W/m^2 in the tropics, from -26 to $+40$ W/m^2 in mid-latitudes, and from -19 to $+35$ W/m^2 in the subarctic. All bulk formulae give smaller δLW than δLW (RTE), the underestimation being larger under dry conditions. Both the Berliand and Bunker formulae, which gave the best agreement with the RTE under both mean conditions and hot and cold conditions, underestimate δLW by as much as 15 W/m^2 in tropical winter and by about 30 W/m^2 in mid-latitudes. The difference between δLW (Hastenrath) and δLW (RTE) is between 10 and 15 W/m^2. The Anderson formula dependence on e_a is the same as that in the Efimova group of formulae and has therefore similar underestimation of δLW compared with the RTE. The Swinbank formula has no explicit dependence on humidity and therefore shows no response to changes in humidity.

5.4. *Remarks*

Based on the results presented so far about $LW\uparrow\downarrow$ under mean and perturbed clear sky conditions, a few statements about the bulk formulae are useful.

Air-sea temperature differences do exist and can be large in certain areas of the ocean, such as the Gulf Stream and the polar oceans. The Brunt and Efimova formulae, which do not include both T_a and T_s dependence, cannot be expected to yield an accurate $LW\uparrow\downarrow$ for all ocean areas. Brunt's formula, with no dependence on T_a, cannot capture $LW\uparrow\downarrow$ changes due to changes in atmospheric temperature. Efimova's formula, with positive correlation between $LW\uparrow\downarrow$ and T_a, has $LW\uparrow\downarrow$ sensitivity to temperature perturbations which is opposite to that expected from radiation physics. Hence neither formula is useful for determining $LW\uparrow\downarrow$.

Because surface humidity observations are not as readily available as surface air temperatures, it is sometimes tempting to calculate $LW\uparrow\downarrow$ from Swinbank's formula which includes an implicit relationship between e_a and T_a. However, air mass characteristics are not uniform over the ocean. We expect that the T_a-e_a relationship of a continental air mass over the Gulf Stream would be very different from that of a maritime air mass over the middle of the Pacific Ocean. Our results for the mean clear sky environments show that LW (Swinbank) is closest to LW (RTE) during winter in the northern hemisphere tropics when the atmospheric conditions assumed are probably most similar to those in southern Australia. Even so, LW (Swinbank) is ~ 6 W/m^2 greater than LW (RTE). The overestimate is as much as 17 W/m^2 in summer in the tropics.

TABLE 6. Like Table 4, Except for Dry Atmospheric Conditions

	15°N		40°N		75°N	
	Summer	Winter	Summer	Winter	Summer	Winter
RTE	23	30	38	40	31	35
Brunt	12	16	21	20	15	15
Berliand	12	16	22	19	16	10
Clark	12	16	21	20	15	15
Hastenrath	10	14	18	18	13	13
Efimova	12	14	15	9	7	1
Bunker	12	15	17	9	7	1
Anderson	11	13	15	8	7	1
Swinbank	0	0	0	0	0	0

Units are in watts per square meter.

TABLE 7. Like Table 4, Except for Wet Atmospheric Conditions

	15°N		40°N		75°N	
	Summer	Winter	Summer	Winter	Summer	Winter
RTE	−17	−23	−26	−21	−19	−13
Brunt	−11	−14	−16	−14	−11	−12
Berliand	−11	−14	−17	−14	−12	−9
Clark	−11	−14	−16	−14	−11	−12
Hastenrath	−9	−12	−14	−12	−10	−11
Efimova	−12	−14	−15	−9	−7	−2
Bunker	−12	−15	−16	−9	−7	−3
Anderson	−11	−13	−15	−9	−7	−2
Swinbank	0	0	0	0	0	0

Units are in watts per square meter.

Hastenrath's formula was developed for and applied to the tropical maritime atmosphere. Thus it seems surprising that even under mean clear sky conditions there, LW (Hastenrath) is greater than LW (RTE) by 10 W/m^2 or more. The humidity dependence in this formula is $-0.056(q_a)^{1/2}$, or $-0.044(e_a)^{1/2}$ (vide (15*b*)). This humidity dependence is smaller than that in the otherwise identical formula used by Clark. Thus for the same surface conditions, the Hastenrath formula yields a larger $LW\uparrow\downarrow$ and shows a smaller sensitivity to humidity perturbations than does the Clark formula. That LW (Hastenrath) has a larger departure from LW (RTE) than LW (Clark) even in the mean tropical environment suggests that the Hastenrath formula may underestimate the effects of humidity on $LW\uparrow\downarrow$.

The remaining four formulae investigated, those of Berliand, Clark, Bunker, and Anderson, all include $LW\uparrow\downarrow$ dependence on T_a, e_a, and T_s. They all yield $LW\uparrow\downarrow$ which are within ± 10 W/m^2 of LW (RTE) under mean clear sky environments in the tropics and at mid-latitudes. Under these conditions it does not matter which formula is used to estimate $LW\uparrow\downarrow$. However, when temperature in the atmospheric column is strongly perturbed, the formulae which have a nonlinear dependence on T_a, i.e., the Berliand, Bunker, and Anderson formulae, yield $LW\uparrow\downarrow$ that are closer to LW (RTE) than the Clark formula with a linear T_a dependence. With negative humidity perturbations in the atmospheric column, all four formulae show δLW value which differ from δLW (RTE) by more than 10 W/m^2. Because δLW (RTE) is asymmetric to symmetric perturbations in humidity, we tend to prefer the Berliand formula which has a square root rather than a linear dependence on e_a.

While the above discussion appears to favor the Berliand formula over the others listed in Table 1*a* to estimate $LW\uparrow\downarrow$ under clear sky conditions, we emphasize that there are limitations of the Berliand formula and that it is not the goal of this study to recommend a particular formula. The Berliand formula does not give accurate $LW\uparrow\downarrow$ under low-humidity conditions or when there is an inversion in the atmosphere, as evidenced by the arctic winter situation and further demonstrated in section 7. Furthermore, the atmosphere over the ocean is seldom completely cloud free. The accuracy of the climatological $LW\uparrow\downarrow$ evaluated from the bulk formulae depends critically on the treatment cloudiness effects in the formulae. This is discussed in the following section.

TABLE 8. Basic Cloud Forms and Their Associated Optical Thicknesses

	Optical Thickness
High Clouds	
Cirrus	<0.5
Cirrostratus	1–4
Middle Clouds	
Cirrocumulus	1–4
Altocumulus	4–8
Altostratus	4–8
Low Clouds	
Nimbostratus	8–>32
Stratocumulus	4–32
Stratus	8–16
Cumulus	4–>32
Cumulonimbus	>32

6. CLOUDY SKY RESULTS

Commonly observed clouds are generally grouped into high, middle, and low clouds to denote the cloud base altitude, i.e., the altitude at which they form. They can also be grouped according to their genera or form. Each cloud form can be further characterized as scattered (when the clear intervals predominate), broken (when the cloud masses predominate), or continuous, thus giving a range of optical thicknesses for each cloud form. The 10 World Meteorological Organization basic cloud forms together with their associated optical thicknesses are listed in Table 8 under their respective height groups.

To isolate the effect of clouds on the instantaneous $LW\uparrow\downarrow$, we assume that the temperature and humidity profiles in the atmosphere are the same as those used in the clear sky investigation. In this way, we do not address the issue of cloud feedback on the atmospheric structure and consequently on $LW\uparrow\downarrow$. Rather, we focus on what $LW\uparrow\downarrow$ might be when a cloud is present in the atmospheric column in which the temperature and humidity profiles are known.

6.1. *RTE Results for Mean Cloudy Sky Conditions*

In this section we use the RTE to investigate the sensitivity of the net longwave radiation at the surface to a hypothetical cloud of given optical thickness occupying one layer in the model (between consecutive symbols in Figures 4–6). Not all the 10 cloud forms can be modeled as a one-layer cloud. The towering cumulonimbus, for example, extends from the condensation level near the surface to the tropopause. However, deep clouds are generally optically black, and their effect on $LW\uparrow\downarrow$ at the surface may be closely given by an optically thick one-layer cloud with the same cloud base conditions.

Figure 3 shows for the mean summer tropical atmosphere the effect of cloud optical thickness on $LW\uparrow\downarrow$, for clouds with cloud bases $P_c = 950$ mbar, 500 mbar, and 200 mbar. $LW\uparrow\downarrow$ at the surface decreases exponentially with cloud optical thickness. A cloud with $\tau_c = 4$ is nearly black in the infrared, and while further increase in τ_c does not represent significant percentage change in $LW\uparrow\downarrow$ at the surface, these changes may be ~ 5 W/m^2. In the discussion in the remainder of this section, we shall use a $\tau_c = 4$ cloud to illustrate the effect of total cloud cover on $LW\uparrow\downarrow$. Figure 4 shows that the effects of clouds of different optical thicknesses are qualitatively similar.

Figure 4 shows that a cloud of $\tau_c = 4$ with cloud base at $P_c = 950$ mbar reduces clear sky $LW\uparrow\downarrow$ by 43 W/m^2 in the mean tropical summer, by 55 W/m^2 in the mean tropical winter, by 57 W/m^2 in the mean mid-latitude summer, by 69 W/m^2 in the mean mid-latitude winter, by 67 W/m^2 in the mean subarctic summer, and by 65 W/m^2 in the mean subarctic winter. These reductions are close to the maximum reduction by a single layer of cloud under mean atmospheric conditions.

As expected, a high cloud has less impact on $LW\uparrow\downarrow$ than a low cloud. The reduction by a cloud with $\tau_c = 4$ and cloud

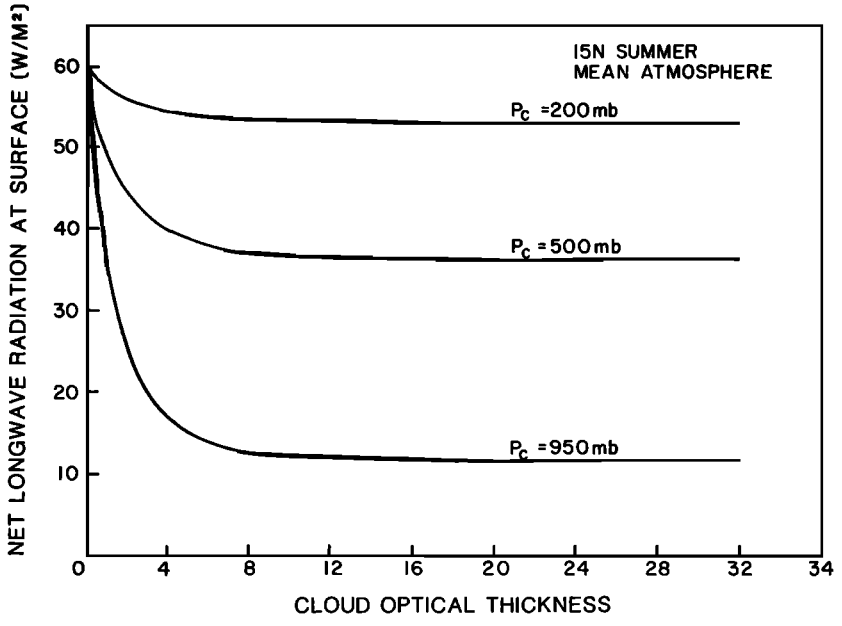

Fig. 3. Variation of net longwave radiation (in watts per square meter) at the ocean surface with cloud optical thickness. It is assumed that atmospheric conditions are typical of the mean summer tropical atmosphere and that a one-layer cloud extends (1) from 950 to 900 mbar, (2) from 500 to 400 mbar, and (3) from 200 to 100 mbar.

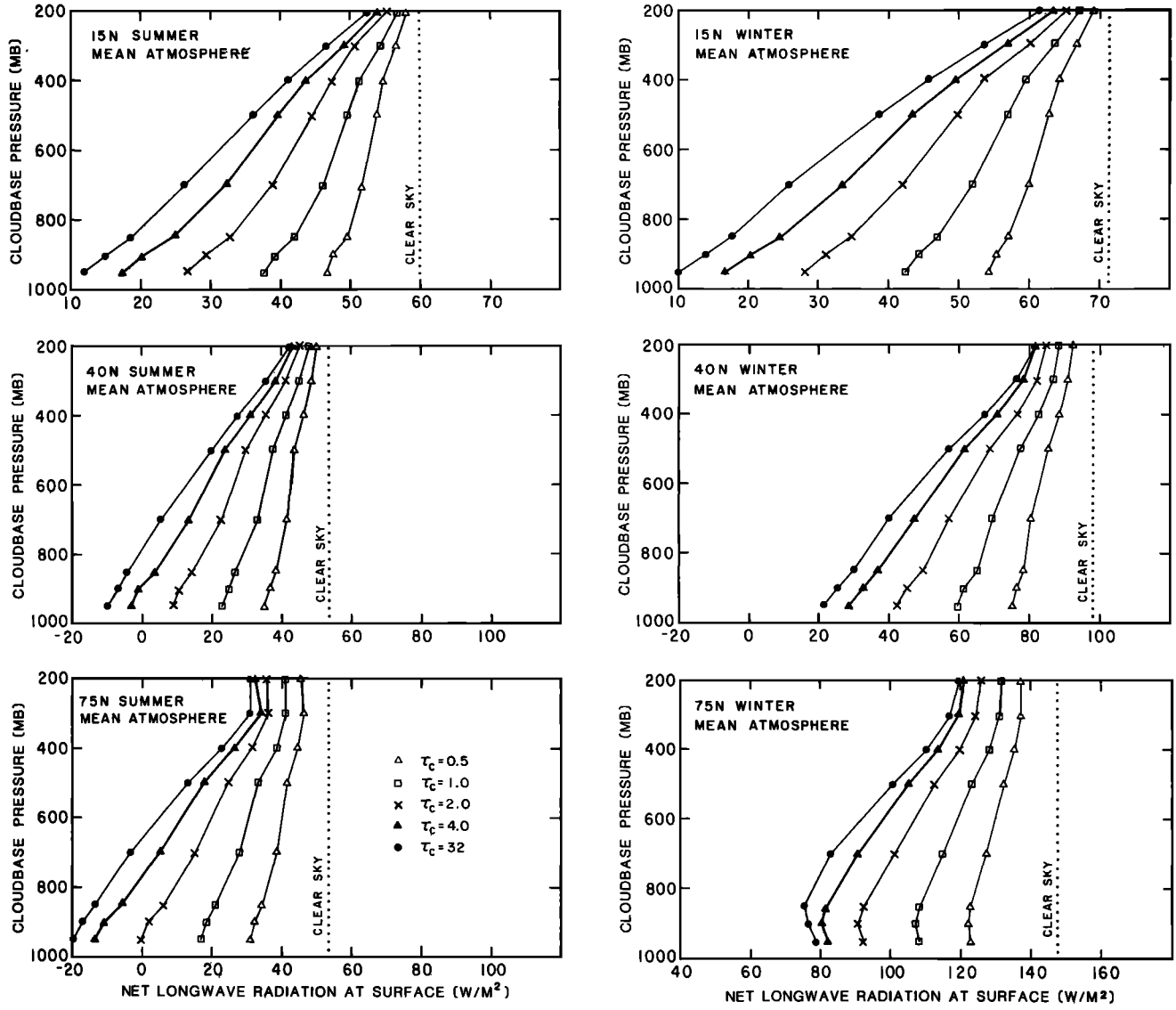

Fig. 4. Variation of net longwave radiation (in watts per square meter) at ocean surface with cloud base pressure and cloud optical thickness. Mean atmospheric conditions are assumed for the six environments. The dotted line indicates the net longwave radiation at the ocean surface under clear skies. A one-layer cloud of optical thickness τ_c is assumed to reside between consecutive symbols.

base at 500 mbar is approximately 50% that by the same cloud with $P_c = 950$ mbar. Thus low, dark clouds cause larger changes in $LW\uparrow\downarrow$ than do 2σ perturbations of the clear sky; 500-mbar cloud base dark clouds cause $LW\uparrow\downarrow$ changes comparable to those due to 2σ perturbations. The same cloud with $P_c = 200$ mbar gives a reduction of ~ 10 W/m^2 in the tropics and mid-latitude summer and ~ 26 W/m^2 in the subarctic winter. While $LW\uparrow\downarrow$ at the surface is less sensitive to the optical thickness of a cloud at 200 mbar than one at a lower altitude, the difference between wispy cirrus ($\tau_c \sim 0.5$) and a cirrus anvil ($\tau_c \sim 4$) may result in a difference of ~ 10 W/m^2 in $LW\uparrow\downarrow$ at the surface.

The observational uncertainty in cloud base can be of consequence, even when the high-, middle-, and low-level categories are used and $T(p)$ and $q(p)$ profiles are known precisely. For example, with mean atmospheric conditions, a shift in cloud base estimate from 500 mbar to 600 mbar will decrease $LW\uparrow\downarrow$ at the surface by 5–10 W/m^2. The uncertainty in $LW\uparrow\downarrow$ due to cloud base altitude is greatest for low clouds; moving a $\tau_c = 4$ cloud from $P_c = 950$ mbar to 900 mbar can change $LW\uparrow\downarrow$ by more than 20 W/m^2.

6.2. *RTE Results for Perturbed Cloudy Sky Conditions*

We next consider the situation when a $\tau_c = 4$ cloud is moved up and down when there are temperature and humidity perturbations in the atmospheric column. These results give information concerning the uncertainty in $LW\uparrow\downarrow$ due to uncertainty in the T-q profiles, for a given cloud location and type. Figure 5 shows the $LW\uparrow\downarrow$ at the surface as a function of cloud base pressure for the five different sets of temperature and humidity profiles for each environment. Under wet or dry conditions, with a $\tau_c = 4$ cloud, $LW\uparrow\downarrow$ at the surface is affected by the integrated humidity between surface and cloud base. Hence uncertainties in humidity conditions under a higher cloud will have a larger impact on $LW\uparrow\downarrow$ than under a

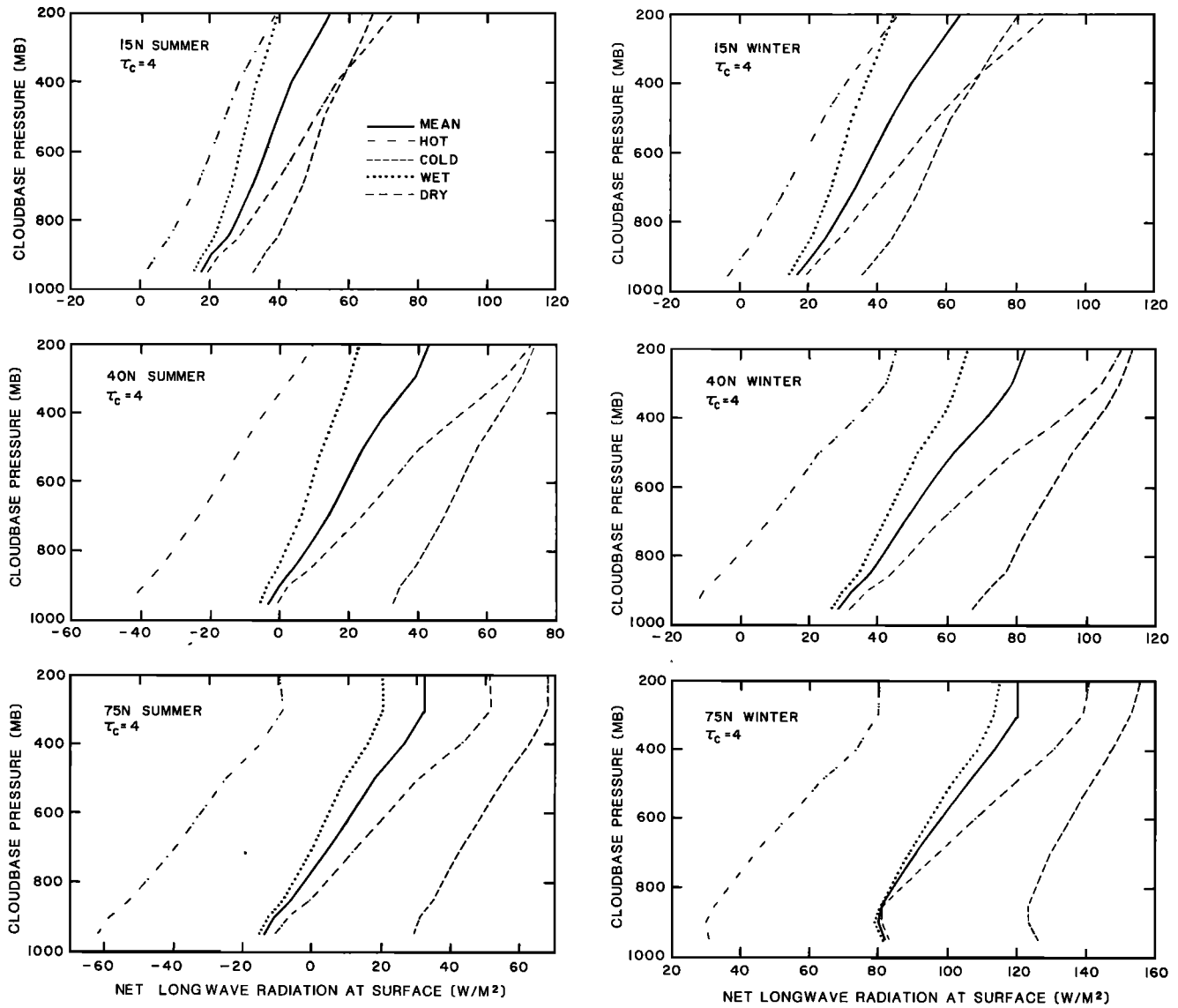

Fig. 5. Variation of net longwave radiation (in watts per square meter) at ocean surface with cloud base pressure and temperature and humidity perturbations in the atmosphere. A one-layer cloud with cloud optical thickness 4 is assumed. The temperature and humidity conditions are given in Figures 2*a* and 2*b*.

lower cloud. Except for high-altitude clouds in the tropics, where the integrated change in humidity to the surface is large, the effect of temperature perturbations is greater than the effect of humidity perturbations on $LW\uparrow\downarrow$.

Figure 5 also shows that, with 100% cloudiness and 2σ perturbations in $T(p)$ or $q(p)$, an instantaneous measurement of $LW\uparrow\downarrow$ at the surface may vary between 2 and 74 W/m^2 in tropical summer, between -3 and 88 W/m^2 in tropical winter, between -44 and 74 W/m^2 in mid-latitude summer, between -14 and 114 W/m^2 in mid-latitude winter, between -62 and 68 W/m^2 in subarctic summer, and between 30 and 156 W/m^2 in subarctic winter. As noted before, these ranges are conservative estimates, since temperature and humidity variations tend to occur concurrently. Nevertheless, these variations are large, much larger than those resulting from changes in the column under clear sky conditions.

6.3. *Bulk Formulae*

Where cloud type information is available, bulk formulae could use cloudiness correction factors for high, middle, and low clouds. Figure 4 shows that this is clearly preferable to a single factor for all cloud types. However, since such information is not yet routinely available and since existing climatologies of $LW\uparrow\downarrow$ have employed single cloudiness factors, it is important to appreciate how well bulk formulae represent $LW\uparrow\downarrow$ under cloudy skies.

From the climatological observations compiled by *Hahn et al.* [1982] and by *Hastenrath and Lamb* [1978] and from the results of the RTE calculations, we see that low clouds account for a significant percentage of all clouds observed in the marine atmosphere and that it is predominantly the atmospheric conditions at and below cloud base that determine $LW\uparrow\downarrow$ at the ocean surface. It thus appears appropriate to use a cloud correction factor derived from surface observations in the bulk formulae to obtain the climatological $LW\uparrow\downarrow$.

The coefficients of $F(C)$ (cf. Table 1*b*) increase poleward. Thus for the same fractional cloud cover C, the "typical" cloud at high latitudes must have larger optical thickness and/or occur at lower altitudes to cause a larger reduction (from clear sky values) in $LW\uparrow\downarrow$ than low-latitude clouds.

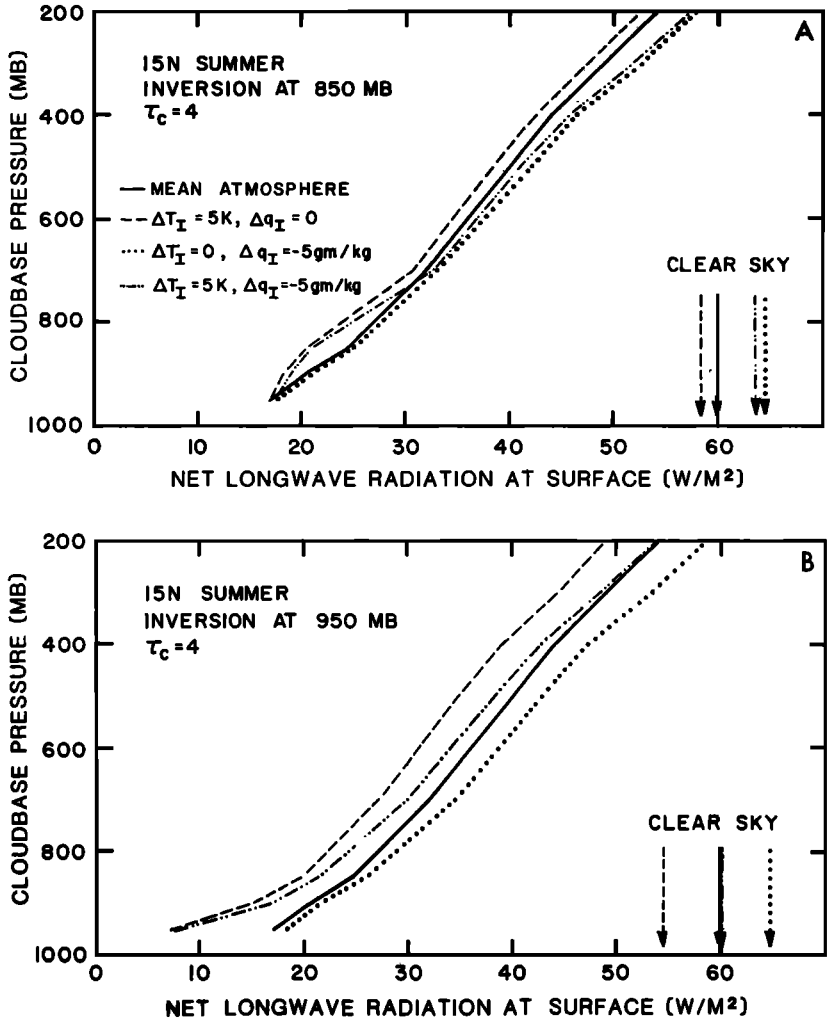

Fig. 6. Variation of net longwave radiation (in watts per square meter) under trade inversions in the summer tropical atmosphere.

Indeed, this north-south trend of the coefficients is supported by the statistics of *Hahn et al.* [1982], which show that the most frequent low cloud at high latitude ocean is stratus ($\tau_c \geq 8$), while that at tropical latitudes is (fair weather) cumulus ($\tau_c \geq 4$).

The statistics of *Hahn et al.* [1982] also show that there are seasonal variations in the frequency of occurrence of each type of low cloud. These seasonal variations are small in comparison with the north-south variations of the frequency of occurrence of each type. It is therefore tempting to conclude that $F(C)$, whose coefficients are seasonally invariant, may be adequate to capture the effect of clouds on $LW\uparrow\downarrow$. The RTE results, however, show that for the same cloud, the percentage reduction of $LW\uparrow\downarrow$ from clear sky values is different for the different environments. Consider a cloud with $\tau_c = 4$ with base at 950 mbar. The percentage reduction of $LW\uparrow\downarrow$ from clear sky values is 72% in tropical summer, 76% in tropical winter, 106% in mid-latitude summer, 70% in mid-latitude winter, 124% in subarctic summer, and 44% in subarctic winter. In other words, even if the "typical" cloud at a latitude had insignificant seasonal variations, its impact on $LW\uparrow\downarrow$ cannot be parameterized by a seasonally invariant cloud correction factor. The mean $LW\uparrow\downarrow$ computed using $F(C)$ can be correct only if the radiative properties of clouds are different seasonally in such a way as to have compensating effects. Unless we have information about the fractional cloud cover, cloud optical thickness as well as frequency distribution of the different types of clouds all over the ocean, we cannot assess how well the bulk formulae represent $LW\uparrow\downarrow$ at the ocean surface.

7. $LW\uparrow\downarrow$ Under an Atmospheric Inversion

Inversions occur in the tropical atmosphere when a convectively unstable boundary layer results from large upward heat flux from the ocean surface. An inversion is typified by a transition region at 950–850 mbar where there is a sharp increase in temperature and a sharp decrease in humidity with height. The inversion generally is capped by a layer of nonprecipitating cumulus clouds. An excellent summary of some observations of the trade wind boundary layer over the Atlantic is given by *Augstein et al.* [1974].

In this section we estimate the $LW\uparrow\downarrow$ at the surface under several inversionlike conditions:

$$\begin{aligned} \Delta T_I &= 5\text{ K} & \Delta q_I &= 0 \\ \Delta T_I &= 0 & \Delta q_I &= -5\text{ g/kg} \\ \Delta T_I &= 5\text{ K} & \Delta q_I &= -5\text{ g/kg} \end{aligned} \tag{16}$$

for inversion heights at $p_I = 950$ mbar and at $p_I = 850$ mbar.

Thus the temperature profile is given by

$$T(p) = \langle T(p) \rangle + \Delta T_I \qquad p = p_I$$
$$= \langle T(p) \rangle \qquad \text{elsewhere} \tag{17}$$

and similarly for $q(p)$.

The effects of ΔT_I and Δq_I on $LW\uparrow\downarrow$ under clear sky conditions are illustrated in the lower right corner of Figures 6*a* and 6*b*. As is to be expected, a higher temperature at p_I increases $LW\downarrow$ and hence reduces $LW\uparrow\downarrow$; conversely, a lower humidity at p_I decreases $LW\downarrow$ and hence increases $LW\uparrow\downarrow$. The net effect of the presence of both the temperature and humidity discontinuities cannot be predicted, however. With $p_I = 850$ mbar the effect of the decreased humidity is greater than the effect of increased temperature, and so $LW\uparrow\downarrow$ under clear sky inversion is 5 W/m^2 larger than the $LW\uparrow\downarrow$ in the mean atmosphere without the inversion. This is similar to the observations of *Reed* [1975] off the coast of Africa. However, with $p_I = 950$ mbar, the temperature and humidity effects nearly cancel, resulting in no observable change in $LW\uparrow\downarrow$ from that in the mean atmosphere.

In the presence of a $\tau_c = 4$ cloud, the largest departure of $LW\uparrow\downarrow$ from mean cloudy atmosphere occurs when the cloud is at the inversion. With nonzero ΔT_I and Δq_I, this departure is ~ 5 W/m^2 with $p_c = p_I = 850$ mbar and is ~ 10 W/m^2 with $p_c = p_I = 950$ mbar.

Recall that the bulk formulae assume that the surface conditions do in some way represent the column mean. In the case of the effects of an inversion (especially when clouds are present), it is clear that such an assumption is incorrect. The surface conditions do not represent the conditions at altitude, and the bulk formulae cannot be expected to estimate $LW\uparrow\downarrow$ accurately.

Inversions occur sufficiently infrequently in the tropics and mid-latitudes, so that no inversion exists in the mean profiles of temperature and humidity (*Oort and Rasmusson* [1971], cf. Figures 1 and 2). However, temperature inversions are so common in the subarctic that the mean subarctic temperature profiles do show inversions. These subarctic inversions, together with the typically low values of e_a there, may account for the relative failure of the bulk formulae $LW\uparrow\downarrow$ to approach that from the RTE.

8. Summary and Conclusions

In this paper we have examined the factors that contribute to the variability of the net longwave radiative fluxes at the ocean surface ($LW\uparrow\downarrow$) by solving the full radiative transfer equations subject to varying conditions in the atmospheric column. The effects of temperature, humidity, and cloud changes on the instantaneous $LW\uparrow\downarrow$ are discussed. The radiative transfer equations are solved by the correlated k distribution method of *Lacis et al.* [1979], which, apart from being computationally efficient, accounts for the vertical inhomogeneity of the atmosphere. The effects of the major and minor gas absorbers as well as of the water vapor continuum are included. Because of the lack of simultaneous observations of longwave radiation at the ocean surface and of the atmospheric column, the radiative transfer model used here has not been validated against actual measurements. However, a comparison of the results from the radiative transfer model with those from a detailed line-by-line calculation shows that model heating/cooling rates are good to at least 1% [*Lacis et al.*, 1979].

The variability of instantaneous $LW\uparrow\downarrow$ is large in comparison with typical climatological mean values. Under clear skies, 2σ perturbations in temperature and specific humidity introduce variations as large as 30 to 40 W/m^2 in $LW\uparrow\downarrow$, the variation being largest under dry conditions. Under cloudy skies, $LW\uparrow\downarrow$ at the surface decreases with increasing cloud optical thickness and with decreasing cloud base altitude. This decrease in $LW\uparrow\downarrow$ from clear sky values may be less than 10 W/m^2 for a thin, high cirrus cloud or as much as 50 to 70 W/m^2 for a towering cumulonimbus. The decrease in $LW\uparrow\downarrow$ caused by low dark clouds is larger than that caused by 2σ perturbations of the clear sky profiles.

Of the eight bulk formulae investigated, our results show that the Bunker, Anderson, and Berliand formulae can reproduce the clear sky mean $LW\uparrow\downarrow$ from the RTE to 10 W/m^2 or better and the clear sky perturbed $LW\uparrow\downarrow$ to 15 W/m^2. Although one or more of the other formulae may work as well for a specific area and season, we prefer Berliand's formula not only for its ability to duplicate the RTE calculations under a wide range of atmospheric conditions, but also for its nonlinear dependence on near-surface air temperature and vapor pressure. However, the sky over the sea is almost never clear, and it is not adequate to choose a bulk formula based on clear sky results.

Because of the strong dependence of $LW\uparrow\downarrow$ on cloud properties, it is impossible to use a single cloudiness factor in the bulk formulae to evaluate the instantaneous $LW\uparrow\downarrow$ at the surface for all cloudy situations; in fact, the bulk formulae were not constructed for such purposes. The latitudinal variation of the constants in the cloud factors cited by *Budyko* [1974] and used by *Clark et al.* [1974] and by *Bunker* [1976] do represent an effort to parameterize, in a simple manner, the longwave radiation response to the "climatological mean cloud" over land at different latitudes. However, we expect the mean cloud statistics over the ocean to be different from those over land. Moreover, there may also be seasonal variation of these mean cloud properties at a latitude. At present there is no global cloud climatology data set adequate to test, with a radiative transfer model, the cloudiness treatment in the bulk formulae. Nor are there enough direct marine observations of $LW\uparrow\downarrow$ to perform a meaningful statistical investigation into the global empirical relationship between oceanic cloudiness and $LW\uparrow\downarrow$. For these reasons, while we have some confidence in the overall patterns and magnitudes of $LW\uparrow\downarrow$ estimated by the bulk formulae, it is not possible to quantify the uncertainties in climatological value of $LW\uparrow\downarrow$ from any of the bulk formulae.

In the coming years we shall rely on satellite-derived observations for information about the atmosphere and the oceans. Our results illustrate the levels of accuracy required of satellite-derived observations of temperature, specific humidity, and cloud properties in the atmosphere to attain a specified accuracy in $LW\uparrow\downarrow$. In order to obtain accuracy of ± 10 W/m^2 in the net longwave radiation at the ocean surface, our results (cf. Figure 5) indicate that the minimum accuracy requirements are ± 2 K for temperature observations and ± 1 g/kg for specific humidity observations at each pressure level, but especially below 500 mbar.

The increasing sophistication of satellite retrieval techniques has made the accuracy requirements for temperature nearly attainable. For water vapor the situation is more difficult. It is generally claimed (see, e.g., *Staelin et al.* [1976]) that the total water vapor amount in the atmospheric column, i.e., the precipitable water, can be measured to within ± 1 g/cm^2. Our results show that this level of accuracy is not adequate. Es-

pecially in the presence of typical low or middle clouds, it is essential to have the distribution, in particular between the surface and cloud base, of specific humidity known to ± 1 g/kg in order to obtain $LW\uparrow\downarrow$ to ± 10 W/m^2.

Our calculations show that uncertainties in $LW\uparrow\downarrow$ due to lack of knowledge about cloud properties is larger than that due to expected uncertainties in temperature or humidity. We need information not only about the fraction of cloud cover, but also about the cloud optical thickness and vertical distribution. The International Satellite Cloud Climatology Project (ISCCP) [*Schiffer and Rossow*, 1983] is now under way to document the global distribution and variation of cloud radiative properties. This data set, when completed, will give us vital information to study the radiative balance at the ocean surface. Even so, retrieval of the vertical distribution of cloud optical thickness (or cloud type information) and cloud base altitude from satellite data are not yet feasible. At present a promising approach might be to use the excellent statistics on the simultaneous occurrence of different cloud types over the ocean [*Hahn et al.*, 1982] and to assume that the bases of low clouds coincide with the lifting condensation level computed from the vertical temperature profile. Unfortunately, no algorithm exists to determine the cloud base altitude of middle clouds. Since our results indicate that an uncertainty of 100 mbar in the base of middle clouds can introduce uncertainties in $LW\uparrow\downarrow$ of at least 10 W/m^2, accurate cloud base determination is essential for an accurate estimate of $LW\uparrow\downarrow$ at the ocean surface.

With the radiative transfer equation and adequate statistics about the atmospheric column, one could derive improved bulk formulae to evaluate the climatological net longwave radiation at the ocean surface. Such bulk formulae probably will require additional atmospheric information beyond T_s, T_a, e_a, and a total cloudiness factor. However, before the formulae can be relied upon to estimate $LW\uparrow\downarrow$ under the wide range of conditions encountered in the atmosphere, we must first have accurate global distributions of temperature, humidity, and cloud properties.

Although $LW\uparrow\downarrow$ is not often one of the dominant terms in the ocean surface energy budget, uncertainties in $LW\uparrow\downarrow$ can hamper energy budget studies as surely as uncertainties in the larger terms; the errors in $LW\uparrow\downarrow$ appear quite plausibly to be up to 50 W/m^2 for a particular monthly average in a given area. The basic physics of the factors that determine $LW\uparrow\downarrow$ is clear, as this study has shown. However, improved determination of $LW\uparrow\downarrow$ will require more data from the atmospheric column than is generally available. Satellite and conventional data will be needed to meet this lack.

APPENDIX: THE CORRELATED k DISTRIBUTION METHOD

Consider a particular gas at a given temperature and pressure. Its absorption coefficient k_ν is a known function of frequency ν. Over some frequency interval, ν to $\nu + \Delta\nu$, k_ν will have considerable structure, which is illustrated schematically in Figure 8*a* of *Hansen et al.* [1983]. From k_ν we can construct the probability distribution function or the "k distribution," $f(k)$, for k_ν in this interval (Figure 8*b* of *Hansen et al.* [1983]). The k distribution $f(k)$ for a given gas and frequency interval $\Delta\nu$ is the probability density function such that $f(k)\,dk$ is the fraction of the frequency interval for which the absorption coefficient is between k and $k + dk$. This is illustrated in Figure 8*b* of *Hansen et al.* [1983].

The k distribution is formally related to the transmission function $T(u)$ by

$$T(u) = \frac{1}{\Delta\nu}\int_{\Delta\nu} e^{-k_\nu u}\,d\nu = \int_0^\infty f(k)e^{-ku}\,dk \qquad \text{(A1)}$$

where u is the gas amount. Since the transmission $T(u)$ or the optical thickness $(k_\nu u)$ are equal for all frequencies with the same absorption coefficient k_ν, it is convenient to group frequencies according to absorption coefficients. To deal with changing line shapes with height, the correlated k distribution method assumes that the k distributions at all altitudes are simply correlated in frequency space, i.e., the strongest absorption occurs at the same frequency at all altitudes and similarly for the weakest absorption.

From $f(k)$ we can determine the cumulative probability function:

$$g(k) = \int_0^k f(k')\,dk' \qquad \text{(A2)}$$

$g(k)$ is the fraction of the interval $\Delta\nu$, such that the absorption coefficient lies between 0 and k. A schematic $g(k)$ is illustrated in Figure 8*c* of *Hansen et al.* [1983]. Let $\{\nu_j\}$ be the set of frequencies such that the absorption coeficients lie between k_j^n and k_{j+1}^n at some level n and between k_j^m and k_{j+1}^m at some other level m. Let these absorption coefficients at level n be ranked so that a fraction g_{j+1} of the frequencies in $\Delta\nu$ have absorption coefficients greater than k_{j+1}^n and a fraction g_j of the frequencies in $\Delta\nu$ have absorption coefficients less than k_j^n. The correlated k distribution method then assumes that at level m the absorption coefficients $k_j^m < k_{j+1}^m$ are similarly ranked, i.e., between g_j and g_{j+1}. In other words, the absorption coefficients associated with the frequencies $\{\nu_j\}$ are always ranged between g_j and g_{j+1}, independent of altitude. In this way the frequency interval $\Delta\nu$ can be partitioned into several sets of frequencies according to the strength of the absorption coefficients. Since $g(k)$ is a monotonic function in k and varies between 0 and 1, satisfactory accuracy and computational speed can be achieved by working with several $g(k)$ or $k(g)$ intervals or frequency groups. In the calculations presented here, eleven k intervals are used for H_2O, ten for CO_2, and four for O_3. The frequencies at which N_2O and CH_4 absorb IR radiation overlap those for H_2O, CO_2, and O_3, and absorption by these trace gases is included in the k intervals for these gases.

For numerical convenience, the *Malkmus* [1967] model is used to represent the transmission

$$T(u) = \exp\left\{-\frac{\pi}{2}B[(1 + 4\,Su/\pi B)^{1/2} - 1]\right\} \qquad \text{(A3)}$$

where the two parameters S and B are the effective line strength and line width. For a given gas and frequency interval, line-by-line absorption at pressures and temperatures over the range encountered in the atmosphere have been computed using the line coefficients tabulated by *McClatchey et al.* [1973] and *Rothman* [1981]. Change of line shape with altitude is accounted for by using the Voigt line profile. Thus a table of S and B parameters is obtained by least squares fitting the Malkmus model to the line-by-line results. The main advantage of using the Malkmus model over other band models

is that the Laplace transform of $T(u)$ (equation (A3)) gives an analytic expression for the k distribution $f(k)$:

$$f(k) = \frac{1}{2} k^{-3/2}(SB)^{1/2} \exp\left[\frac{\pi}{4} B\left(2 - \frac{k}{S} - \frac{S}{k}\right)\right] \quad \text{(A4)}$$

which can be integrated analytically to give the cumulative probability

$$g(k) = \int_0^k f(k')\, dk' \quad \text{(A5)}$$

This permits convenient numerical subdivision of the probability distribution for efficient computation.

Correlated absorption coefficients $k(g)$ are then obtained from (A3) to (A5) for each layer of the atmosphere. The corresponding transmission functions are spectrally weighted by the Planck function for the frequencies in $\{\nu_j\}$ to yield $E_{j,n}{}^{\uparrow}$ and $E_{j,n}{}^{\downarrow}$. It follows that $U_{\nu,n}$ and $D_{\nu,n}$ in (6) to (12) then become $U_{j,n}$ and $D_{j,n}$, the upward and downward irradiances for the group of frequencies $\{\nu_j\}$ where the optical thickness is $\tau_{j,n}$. After integration over height, the upward and downward fluxes are summed over all k intervals. Three quadrature points are used to integrate over the angular distribution of the radiation field to yield the total upward and downward fluxes at each level.

The accuracy of this method depends of course on the validity of the correlated k distribution method and on the number of k intervals used. The maintenance of the ranking of absorption coefficients throughout the atmosphere is rigorously correct for a single spectral line with a fixed center and for a uniform *Elsasser* [1942] band model. Some blurring of the assumed correlation must occur for a real absorption spectrum, owing to overlapping of lines with differing strengths and temperature dependence.

Acknowledgments. We thank E. S. Sarachik and W. B. Rossow for many stimulating discussions and the reviewers for their helpful comments. J. Forkosh assisted in the initial efforts to use the radiation package. D. Smith typed the manuscript, and L. DeValle and J. Mendoza drafted the figures. This work was supported by NASA Cooperative agreement NCC 5-16 Task II (I.F.) and by NASA grant NGT-22-009-900 and National Science Foundation grant OCE-83-01787 to Massachusetts Institute of Technology (D.E.H.).

REFERENCES

Alexander, R. C., and R. L. Mobley, Monthly average sea-surface temperature and ice-pack limits on a 1° global grid, *Mon. Weather Rev.*, *104*, 143–148, 1976.

Anderson, E. R., Energy budget studies, *U.S. Geol. Surv. Circ.*, *229*, 71–119, 1952.

Augstein, E., H. Schmidt, and F. Ostapoff, The vertical structure of the atmospheric planetary boundary layer in undisturbed trade winds over the Atlantic Ocean, *Boundary Layer Meteorol.*, *6*, 129–150, 1974.

Berliand, M. E., and T. G. Berliand, Measurement of the effective radiation of the earth with varying cloud amounts (in Russian), *Izv. Akad. Nauk SSSR Ser. Geofiz.*, no. 1, 1952.

Brunt, D., Notes on radiation in the atmosphere, *Q. J. R. Meteorol. Soc.*, *58*, 389–420, 1932.

Brunt, D., *Physical and Dynamical Meteorology*, 428 pp., Cambridge University Press, New York, 1939.

Budyko, M. I., *Guide to the Atlas of the Heat Balance of the Earth, Publ. WB/T-106*, translated from Russian by I. A. Donehoo, U.S. Weather Bureau, Washington, D. C., 1964.

Budyko, M. I., *Climate and Life*, 508 pp., Academic, New York, 1974.

Bunker, A. F., Computation of surface energy flux and annual air-sea cycle of the North Atlantic Ocean, *Mon. Weather Rev.*, *104*, 1122–1140, 1976.

Clark, N. E., L. Eber, R. M. Laurs, J. A. Renner, and J. F. T. Saur, Heat exchange between ocean and atmosphere in the eastern North Pacific for 1961–71, *NOAA Tech. Rep. NMFS SSRF-682*, U.S. Dep. of Commer., Washington, D. C., 1974.

Duing, W., F. Ostapoff, and J. Merle, *Physical Oceanography of the Tropical Atlantic During GATE*, 117 pp., University of Miami, Miami, Fla., 1980.

Efimova, N., Values of total net longwave radiation at several points in the USSR (in Russian), *Meteorol. Gidrol.*, *5*, 1939.

Efimova, N. A., On methods of calculating monthly values of net longwave radiation (in Russian), *Meteorol. Gidrol.*, *10*, 28–33, 1961.

Elsasser, W. M., Heat transfer by infrared radiation in the atmosphere, in *Harvard Meteorology Studies*, no. 6, 107 pp., Harvard University Press, Cambridge, Mass., 1942.

Galperin, B. M., The net radiation at the Lower Volga during the warm season (in Russian), *Leningrad Gl. Geofiz. Obs. Tr.*, no. 18, 1949.

Gautier, C., G. Diak, and S. Masse, A simple physical model to estimate incident solar radiation at the surface from GOES satellite data, *J. Appl. Meteorol.*, *19*, 1005–1012, 1980.

Hahn, C. J., S. G. Warren, J. London, R. M. Chervin, and R. Jenne, Atlas of simultaneous occurrence of different cloud types over the ocean, *NCAR Tech. Note 201 TSTR*, Natl. Center for Atmos. Res., Boulder Colo., 1982.

Hansen, J., and L. Travis, Light scattering in planetary atmospheres, *Space Sci. Rev.*, *16*, 527–610, 1974.

Hansen, J., et al., Efficient three dimensional global models for climate studies: Models I and II, *Mon. Weather Rev.*, *111*, 609–662, 1983.

Hastenrath, S., and P. J. Lamb, *Heat Budget Atlas of the Tropical Atlantic and Eastern Pacific Oceans*, 90 pp., The University of Wisconsin Press, Madison, 1978.

Houghton, J. T., *The Physics of Atmospheres*, 203 pp., Cambridge University Press, New York, 1977.

Keeling, C. D., The global carbon cycle: What we know and could know from atmospheric, biospheric, and oceanic observations, in *Proceedings: Carbon Dioxide Research Conference: Carbon Dioxide, Science and Consensus, Publ. CONF-820970*, U.S. Department of Energy, Washington, D. C., 1982.

Kondrateyev, K. Ya., *Radiation in the Atmosphere*, 912 pp., Academic, New York, 1969.

Lacis, A. A., and J. E. Hansen, A parameterization for the absorption of solar radiation in the earth's atmosphere, *J. Atmos. Sci.*, *31*, 118–133, 1974.

Lacis, A. A., W.-C. Wang, and J. E. Hansen, Correlated k-distribution method for radiative transfer in climate models: Application to effect of cirrus clouds on climate, *NASA Conf. Publ.*, *2076*, 309–314, 1979.

Levastu, T., Cloud factor in longwave radiation formulae, *J. Geophys. Res.*, *72*, 4277, 1967.

Liou, K. N., *An Introduction to Atmospheric Radiation*, Academic, New York, 1980.

Malkmus, W., Random Lorentz band model with exponential-tailed S^{-1} line intensity distribution function, *J. Opt. Soc. Am.*, *57*, 323–329, 1967.

McClatchey, R. A., et al., AFCRL atmospheric absorption line parameters compilation, *AFCRL-TR-73-0096, Environ. Res. Pap. 434*, Air Force Cambridge Res. Lab., Bedford, Mass., 1973.

Miyakoda, K., and A. Rosati, The variation of sea surface temperature in 1976 and 1977, 1, The data analysis, *J. Geophys. Res.*, *87*, 5667–5680, 1982.

Niiler, P. P. (Ed.), *Tropic Heat, A Study of the Tropical Pacific Upper Ocean Heat, Mass and Momentum Budgets*, Scripps Institution of Oceanography, La Jolla, Calif., 1982.

Oort, A., and E. Rasmusson, *Atmospheric Circulation Statistics, NOAA Prof. Pap. 5*, 323 pp., U.S. Department of Commerce, Washington, D. C., 1971.

Oort, A., and T. H. Vonder Haar, On the observed annual cycle in the ocean atmosphere heat balance of the northern hemisphere, *J. Phys. Oceanogr.*, *6*, 781–800, 1976.

Park, J. H., and J. London, Ozone photochemistry and radiative heating of the middle atmosphere, *J. Atmos. Sci.*, *31*, 1898–1916, 1974.

Reed, R. K., Variation in oceanic net longwave radiation caused by atmospheric thermal structure, *J. Geophys. Res.*, *80*, 3819–3820, 1975.

Reed, R. K., An estimation of net longwave radiation from the oceans, *J. Geophys. Res.*, *81*, 5793–5794, 1976.

Reed, R. K., and D. Halpern, Insolation and net longwave radiation off the Oregon coast, *J. Geophys. Res.*, *80*, 839–844, 1975.

Rothman, L. S., AFGL atmospheric absorption line parameters com-

pilation: 1980 version, *Appl. Opt.*, *20*, 791–794, 1981.
Schiffer, R. A., and W. B. Rossow, The International Satellite Cloud Climatology Project (ISCCP): The first project of the World Climate Research Programme, *Bull. Am. Meteorol. Soc.*, *64*, 779–784, 1983.
Simpson, J. J., and C. A. Paulson, Mid-ocean observations of atmospheric radiation, *Q. J. R. Meteorol. Soc.*, *105*, 482–502, 1979.
Staelin, D. H., et al., Remote sensing of atmospheric water vapor and liquid water with Nimbus 5 spectrometer, *J. Appl. Meteorol.*, *15*, 1204–1214, 1976.
Stephens, G. L., G. G. Campbell, and T. H. Vonder Haar, Earth radiation budgets, *J. Geophys. Res.*, *86*, 9739–9760, 1981.
Swinbank, W. C., Longwave radiation from clear skies, *Q. J. R. Meteorol. Soc.*, *89*, 339–348, 1963.
Tiwari, S. N., Models for infrared atmospheric radiation, in *Advances in Geophysics*, vol. 20, edited by B. Saltzman, 307 pp., Academic, New York, 1978.
Weare, B. C., and P. T. Strub, The significance of sampling biases on calculated monthly mean oceanic surface heat fluxes, *Tellus*, *33*, 211–224, 1981.
Wyrtki, K., The average annual heat balance of the North Pacific Ocean and its relation to ocean circulation, *J. Geophys. Res.*, *70*, 4547–4559, 1965.

I. Y. Fung and A. A. Lacis, NASA Goddard Space Flight Center, Institute for Space Studies, 2880 Broadway, New York, NY 10025.
D. E. Harrison, Center for Meteorology and Physical Oceanography, Massachusetts Institute of Technology, Cambridge, MA 02139.

(Received May 11, 1983;
revised January 5, 1984;
accepted February 8, 1984.)